

A test for stationarity of spatio-temporal random fields on planar and spherical domains

Mikyong Jun and Marc G. Genton¹

April 6, 2011

ABSTRACT: A formal test for weak stationarity of spatial and spatio-temporal random fields is proposed. We consider the cases where the spatial domain is planar or spherical and we do not require distributional assumptions for the random fields. The method can be applied to univariate or to multivariate random fields. Our test is based on the asymptotic normality of certain statistics that are functions of estimators of covariances at certain spatial and temporal lags under weak stationarity. Simulation results for spatial as well as spatio-temporal cases on the two types of spatial domains are reported. We describe the results of two applications of the proposed method. One is to test stationarity of Pacific wind data. The other is to test axial symmetry of climate model errors for surface temperature using the NOAA GFDL model outputs and the observations from the Climate Research Unit in East Anglia and the Hadley Centre.

KEY WORDS: Asymptotic normality; Axial symmetry; Climate model output; Increasing domain asymptotics; Inference; Pacific wind data; Stationarity

¹Department of Statistics, Texas A&M University, College Station, TX 77843-3143 (E-mail: {mjun,genton}@stat.tamu.edu). The authors acknowledge support from NSF grant ATM-0620624. Mikyong Jun's research is also supported by NSF grant DMS-0906532. Marc Genton's research is also supported by NSF grant DMS-1007504. This research is partially supported by Award No. KUS-C1-016-04, made by King Abdullah University of Science and Technology (KAUST). The authors acknowledge the modeling groups for making their simulations available for analysis, the Program for Climate Model Diagnosis and Intercomparison (PCMDI) for collecting and archiving the CMIP3 model output, and the World Climate Research Programme (WCRP)'s Working Group on Coupled Modelling (WGCM) for organizing the model data analysis activity. The WCRP CMIP3 multi-model dataset is supported by the Office of Science, U.S. Department of Energy. The authors thank Nikolay Bliznyuk, Suhasini Subba Rao, an Associate Editor, and two anonymous referees for their valuable comments that helped to improve the manuscript.

1. INTRODUCTION

When dealing with spatial or spatio-temporal data from environmental applications, one often makes simplifying assumptions on the covariance structure, such as stationarity. For a spatial random field, $Z(\mathbf{s})$, defined in $D \subset \mathbb{R}^d$, we say that it is (weakly) stationary if the mean is constant across the spatial domain, D , and the covariance only depends on the lag between two spatial locations. That is, $E\{Z(\mathbf{s})\} = \mu \in \mathbb{R}$ for all $\mathbf{s} \in D$ and $\text{Cov}\{Z(\mathbf{s}_1), Z(\mathbf{s}_2)\} = C(\mathbf{s}_1 - \mathbf{s}_2)$ for an autocovariance function C and for all $\mathbf{s}_1, \mathbf{s}_2 \in D$. Therefore, if a spatial random field is nonstationary, the nonstationarity may be present in the mean and/or the covariance structure. In this paper, we focus on the nonstationarity of the random field in the covariance structure assuming the mean of the random field is zero. If the random field does not have zero mean, we assume that we can remove the mean structure by subtracting a proper estimate of it and get a zero mean random field.

For a spatial random field defined in \mathbb{R}^d or a spatio-temporal random field defined in $\mathbb{R}^d \times \mathbb{Z}$ ($d \geq 1$), several authors have developed various stationary or isotropic covariance models; see Gneiting, Genton, and Guttorp (2007) for a recent review. There also have been a number of papers that discuss hypothesis tests on separability of spatio-temporal covariance structure (Mitchell, Genton, and Gumpertz 2005, 2006; Fuentes 2006; Bevilacqua, Mateu, Porcu, Zhang, and Zini 2010). However, there are only few papers that discuss hypothesis tests of stationarity. Fuentes (2005) presented a test of stationarity for spatial random fields through a direct extension of the test of stationarity for time series by Priestley and Subba Rao (1969). The idea is based on spatial spectral analysis, but this approach requires that the spatial random field is on a regular grid. Dwivedi and Subba Rao (2010) developed a test of stationarity for time series based on the Discrete Fourier Transform but their asymptotic distribution of the test statistic is derived under the assumption that the process is either $\text{MA}(\infty)$ or is strongly stationary under some mixing conditions.

If the data cover a large portion of the Earth, as it is commonly the case for satellite data or numerical model outputs, we need to consider a random field on the surface of the sphere. In this case the stationarity of the random field should be defined in a different way. If the random field on the surface of the sphere is isotropic, similarly to a random field in \mathbb{R}^d , the covariance between two locations on the surface of the sphere should depend on the two locations only through the distance on the surface of the sphere. However, the usual distance measure on the sphere, i.e., the great

circle distance or the chordal distance, is a function of the two latitude points, and the longitudinal lag. For example, the chordal distance between two locations on a globe, (L_i, l_i) , $i = 1, 2$ (L_i : latitude, l_i : longitude), is given by

$$\text{ch}(L_1, L_2, l_1 - l_2) = 2R \left\{ \sin^2 \left(\frac{L_1 - L_2}{2} \right) + \cos L_1 \cos L_2 \sin^2 \left(\frac{l_1 - l_2}{2} \right) \right\}^{1/2}.$$

Here, R is the radius of the Earth. The great circle distance between the two locations is $\text{gc}(L_1, L_2, l_1 - l_2) = 2R \arcsin\{\text{ch}(L_1, L_2, l_1 - l_2)/(2R)\}$. Therefore unlike in the Euclidean domain, even if the random field is isotropic, it may not imply that the random field is stationary in latitude, unless the longitudinal lag is zero.

It is commonly found that global data from environmental applications exhibit strong dependence of the covariance on latitude (e.g. Stein (2007) and Jun and Stein (2008)). This is not mainly due to the fact that distance on a sphere is a function of two latitude points, since usually it is the case that the covariance structures in the Northern and Southern Hemispheres are not symmetric around the Equator (if the random field is isotropic, the covariance structure should be symmetric around the Equator). For example, the left panel of Figure 1 shows the standard deviation of global surface temperature data (specifically, the difference between the temperature observation and climate model output for the corresponding quantity, see Section 5.2 for more details on the data) with respect to latitude. The dependence of the standard deviation of the data on latitude is not symmetric around the Equator. Therefore, it is sometimes assumed that the random field is not isotropic, but stationary with respect to longitude (and time) and nonstationary with respect to latitude. For a global random field $Z(L, l)$ (L : latitude, l : longitude) on a sphere, we say that Z is *axially symmetric* if the covariance only depends on longitude through the difference between the two longitude values (Jones 1963): $\text{Cov}\{Z(L_1, l_1), Z(L_2, l_2)\} = C(L_1, L_2, l_1 - l_2)$ for all L_1, L_2, l_1, l_2 and an appropriate covariance function C . The covariance models used in Stein (2007), and Jun and Stein (2007, 2008) are not isotropic and they assume axial symmetry.

The motivation of this work comes from the axial symmetry assumption used for random fields on a sphere. In Figure 1, the dependence of the standard deviation of the data on latitude is apparent although such dependence on longitude is much weaker. Stein (2007) and Jun and Stein (2008) showed similar features for the total column ozone concentration data and concluded that the axial symmetry assumption for the data is reasonable. Similarly, Cressie and Huang (1999) examined several empirical pictures of standard deviations and variograms and concluded that

there was no clear nonstationarity in the Pacific wind data (see Section 5.1 about the data). In all of the above examples, however, the judgment on whether or not the random field is stationary (or axially symmetric for random fields on a sphere) is subjective and mostly based on some empirical plots of covariances or variograms.

Our goal in this paper is to present a formal hypothesis test for stationarity or axial symmetry of spatial and spatio-temporal random fields on both planar and spherical domains. Recently, there has been a series of papers that have developed tests for various properties of the covariance structure for spatial and spatio-temporal random fields based on empirical covariance estimators as test statistics. Guan, Sherman, and Calvin (2004) developed a test for isotropy of a spatial random field in \mathbb{R}^2 using the asymptotic joint normality of empirical covariance estimators at several spatial lags. Li, Genton, and Sherman (2007, 2008a,b) extended this idea to test separability and full symmetry for spatio-temporal random fields in both univariate and multivariate cases. Li et al. (2009) tested the Taylor's hypothesis for the space-time covariance structure of rainfall data. However, all of these results may not be applied directly to our situation for the following reasons. First, the results in Guan et al. (2004), Li et al. (2007, 2008a,b), and Li et al. (2009) are based on the assumption that the underlying spatial or spatio-temporal random fields are strongly stationary. In our case, we test weak stationarity and thus we need to develop the theory without the assumption of strong stationarity on the random fields. Second, we consider random fields not only on planar domains but also on spherical domains. One of the main applications that we have is testing the covariance structure of global data. Therefore, although the present work builds upon the existing results in Guan et al. (2004) and Li et al. (2008a,b), there are some significant differences.

The rest of the paper is organized as follows. Section 2 develops the asymptotic joint normality of our test statistics with some moment and mixing conditions. We consider spatial and spatio-temporal random fields as well as planar and spherical domain cases. The formal testing procedure is presented in Section 3. We report simulation results in Section 4. The application results to the Pacific Ocean wind data and global temperature data are given in Section 5. We conclude the paper with some discussions and the proof of the theorem is given in the Appendix.

2. ASYMPTOTIC THEORY

We test weak stationarity of spatial and spatio-temporal random fields on either planar or spherical domains. The basic idea is to divide the spatial domain into two (or more) disjoint domains

and use the test statistic that is based on the difference between empirical estimators of covariances at given lags from the disjoint spatial sub-domains. We establish the asymptotic normality of the empirical estimators and we use an asymptotic chi-squared test based on it.

We divide the problem into several different cases. We firstly separate the cases depending on whether the random field is spatial or spatio-temporal. Then, for each case, we consider planar spatial domains and spherical spatial domains separately. For planar spatial domains, the asymptotic results are based on increasing domain asymptotics. For the spatio-temporal case, we assume that the spatial domain is fixed and the asymptotics come from the increasing time domain. We then discuss how the results can be extended to multivariate random fields.

We denote the random field as $Z(\mathbf{x})$. If we consider a spatial random field, $\mathbf{x} = \mathbf{s} \in D$ where D is the spatial domain. If we consider a spatio-temporal random field, $\mathbf{x} = (\mathbf{s}, t) \in D \times \mathbb{Z}$. In particular, if we consider a spatial random field on a sphere, we may let $\mathbf{x} = (L, l) \in D \subset \mathcal{S}^2$, where L denotes the latitude, l the longitude, and \mathcal{S}^2 the surface of a sphere with radius R in \mathbb{R}^3 . We also introduce a general notation for the lag, \mathbf{k} , such that this may contain either spatial ($\mathbf{k} = \mathbf{h}$) or spatio-temporal ($\mathbf{k} = (\mathbf{h}, u)$) lags depending on the case under study.

2.1 Spatial random fields

We first suppose that the observations are taken over $D \subset \mathbb{R}^d$ for some $d \geq 1$. Guan et al. (2004) dealt with the case $d = 2$, and we also present the results for $d = 2$, but it is easy to show that our results hold for general $d \geq 1$. We consider a regularly spaced domain in this case. Similar results may hold for irregularly spaced cases along the same line as considered by Guan et al. (2004) for that setting. We assume that the spatial domain is increasing and the asymptotic results come from increasing domain asymptotics.

Consider a spatial random field $\{Z(\mathbf{s}) : \mathbf{s} \in D\}$. Suppose the observations are taken over $D \subset \mathbb{Z}^2$, a 2-dimensional space of integer lattice points. We assume Z has mean zero. If Z has non-zero mean, the results are the same as long as we use Z after removing the fixed mean part. We denote the covariance function of Z as $C(\mathbf{s}, \mathbf{s} + \mathbf{h}) = \text{Cov}\{Z(\mathbf{s}), Z(\mathbf{s} + \mathbf{h})\}$, where $\mathbf{s}, \mathbf{s} + \mathbf{h} \in D$. In the case that the random field Z is weakly stationary, $C(\mathbf{s}, \mathbf{s} + \mathbf{h}) = C(\mathbf{0}, \mathbf{h}) = C_0(\mathbf{h})$ for all $\mathbf{s} \in D$, \mathbf{h} , and a stationary covariance function C_0 . Now denote $S(\mathbf{h}; D) = \{\mathbf{s} : \mathbf{s} \in D, \mathbf{s} + \mathbf{h} \in D\}$ and let $|S(\mathbf{h}; D)|$

be the cardinality of $S(\mathbf{h}; D)$. We consider a statistic calculated from Z ,

$$\widehat{A}(\mathbf{h}; D) = \frac{1}{|S(\mathbf{h}; D)|} \sum_{\mathbf{s} \in S(\mathbf{h}; D)} Z(\mathbf{s})Z(\mathbf{s} + \mathbf{h}). \quad (1)$$

If Z is weakly stationary with the covariance function C_0 such that $C_0(\mathbf{h}) = \text{Cov}\{Z(\mathbf{s}), Z(\mathbf{s} + \mathbf{h})\}$, then $\widehat{A}(\mathbf{h}; \cdot)$ is an estimator of the covariance $C_0(\mathbf{h}) = C(\mathbf{0}, \mathbf{h})$ for a spatial lag \mathbf{h} .

First we discuss the spatial domain and its shape. Our test is based on the statistic using the difference of estimators from two disjoint spatial domains whose union is the entire domain. That is, we let D_n be the entire domain that increases as n increases and we consider $D_{n,1}$ and $D_{n,2}$ such that $D_{n,1} \sqcup D_{n,2} = D_n$ (\sqcup denotes a union of disjoint sets). We also require $\frac{|D_{n,1}|}{|D_{n,2}|} = O(1)$. An example of a spatial domain when $d = 2$ may be the one given in Guan et al. (2004): let $B \subset (0, 2] \times (0, 1]$ be the interior of a simple closed curve such that $B \cap (0, 1] \times (0, 1]$ and $B \cap (1, 2] \times (0, 1]$ have nonempty interiors. Then multiply the set B by n and obtain $B_n \subset (0, 2n] \times (0, n]$. We define $D_n = \{\mathbf{s} : \mathbf{s} \in B_n \cap \mathbb{Z}^2\}$, $D_{n,1} = D_n \cap (0, n] \times (0, n]$, and $D_{n,2} = D_n \cap (n, 2n] \times (0, n]$. The shape of D_n may be more general than the above formulation but in general, we require

$$|D_n| = O(n^2) \text{ and } |\partial D_n| = O(n) \quad (2)$$

where we define the boundary of a set D to be the set $\partial D \equiv \{\mathbf{s} \in D : \exists \mathbf{s}' \notin D \text{ s.t. } d(\mathbf{s}, \mathbf{s}') = 1\}$, where $\mathbf{s} = (s_x, s_y)^T$, $d[(s_x, s_y), (s'_x, s'_y)] \equiv \max(|s_x - s'_x|, |s_y - s'_y|)$ and $|\partial D|$ denotes the number of points in ∂D .

For a set of spatial lags Λ , define $\widehat{\mathbf{G}}_{n,i} = \{\widehat{A}(\mathbf{h}; D_{n,i}) : \mathbf{h} \in \Lambda\}$ for $i = 1, 2$. If we assume Z is strongly stationary, the asymptotic normality of $\widehat{\mathbf{G}}_{n,i}$ follows directly from the result in Guan et al. (2004). However, several assumptions required in Guan et al. (2004) may not be relevant in our case since the random field that we start with may be neither strongly nor weakly stationary. In the following, we discuss the assumptions that we require for the test. In addition, we establish the asymptotic joint normality of $\widehat{\mathbf{G}}_n = (\widehat{\mathbf{G}}_{n,1}, \widehat{\mathbf{G}}_{n,2})^T$ in this section.

To achieve asymptotic joint normality of $\widehat{\mathbf{G}}_n$, we require the following assumptions. First, let

$$\alpha(p, k) \equiv \sup\{|P(A_1 \cap A_2) - P(A_1)P(A_2)| : A_i \in \mathcal{F}(E_i), |E_i| \leq p, i = 1, 2, d(E_1, E_2) \geq k\},$$

where $|E|$ is the cardinality of the index set E , $\mathcal{F}(E)$ is the σ -algebra generated by the random variables $\{Z(\mathbf{s}) : \mathbf{s} \in E\}$ and $d(E_1, E_2)$ is the minimal ‘‘city block’’ distance between E_1 and E_2 .

Then we assume

$$\sup_p \frac{\alpha(p, k)}{p} = O(k^{-\epsilon}) \text{ for some } \epsilon > 2. \quad (3)$$

The condition (3) implies that as the distance k increases, the dependence decreases at a polynomial rate in k . Guan et al. (2004) and Li et al. (2008a) assume the same mixing condition. Any m -dependent random field (observations separated by a distance larger than m are independent) satisfies this condition.

We may need the following moment condition for the case of a general random field Z (that may be nonstationary),

$$\sup_n E\{|\sqrt{|D_{n,i}|} \times |\hat{A}(\mathbf{h}; D_{n,i})|^{2+\delta}\} \leq C_\delta \quad (4)$$

for some $\delta > 0$, $C_\delta < \infty$ and $i = 1, 2$. Guan et al. (2004) require a similar moment condition for an empirical variogram estimator of a strongly stationary random field. The condition in (4) is required to show the asymptotic joint normality of $\hat{\mathbf{G}}_n$ and is only slightly stronger than the existence of the (standardized) asymptotic variance of $\hat{A}(\mathbf{h}; D_{n,i})$. We may also require $\lim_{n \rightarrow \infty} \sqrt{|D_{n,i}| |D_{n,j}|} \text{Cov}\{\hat{A}(\mathbf{h}_1; D_{n,i}), \hat{A}(\mathbf{h}_2; D_{n,j})\}$ to exist and be finite for $i, j = 1, 2$ and $\mathbf{h}_1, \mathbf{h}_2 \in \Lambda$. This holds if we have

$$\sum_{\mathbf{s}_1 \in S(\mathbf{h}_1; D_{n,i})} \sum_{\mathbf{s}_2 \in S(\mathbf{h}_2; D_{n,j})} \text{Cov}\{Z(\mathbf{s}_1)Z(\mathbf{s}_1 + \mathbf{h}_1), Z(\mathbf{s}_2)Z(\mathbf{s}_2 + \mathbf{h}_2)\} = O(n^2) \quad (5)$$

for $i, j = 1, 2$. This condition (5) holds for any m -dependent process with finite fourth moment. Also this condition should hold if $E\{|Z(\mathbf{s})|^{4+\delta}\} < D_\delta$ for some $\delta > 0$ and $D_\delta < \infty$.

Theorem 1. *Let $\{Z(\mathbf{s}) : \mathbf{s} \in \mathbb{Z}^d\}$ be a random field that is observed in D_n satisfying (2). If the condition (5) holds, then the block matrix $\Sigma = (\Sigma_{ij})$, where $\Sigma_{ij} \equiv \lim_{n \rightarrow \infty} \frac{1}{4} |D_n| \text{Cov}(\hat{\mathbf{G}}_{n,i}, \hat{\mathbf{G}}_{n,j})$, $i, j = 1, 2$, exists and is finite. If we further assume that Σ , Σ_{11} , Σ_{22} are positive definite, that the conditions (3) and (4) hold, and that Z is weakly stationary with autocovariance function C_0 and if we denote $\mathbf{G} = \{C_0(\mathbf{h}) : \mathbf{h} \in \Lambda\}$, then the limiting distribution of $(\sqrt{|D_{n,1}|}(\hat{\mathbf{G}}_{n,1} - \mathbf{G}), \sqrt{|D_{n,2}|}(\hat{\mathbf{G}}_{n,2} - \mathbf{G}))^T$ is multivariate normal with mean zero and covariance matrix Σ .*

Proof. See the Appendix.

For the spatial case with a spherical domain, a natural asymptotic framework is the so called fixed domain asymptotics or infill asymptotics (Stein 1995; Lahiri 1996; Zhang and Zimmerman

2005), since it is natural to assume that the radius R of the sphere is fixed. To the best of our knowledge, there has been no results on the asymptotic properties of statistics as in (1) under an infill asymptotics framework on the sphere. While we suspect that a similar asymptotic normality might hold under infill asymptotics with appropriate conditions, it remains an open problem.

2.2 Spatio-temporal random fields

The argument for this case is similar to the one in Section 2.1 but we do not make any assumption (such as increasing, infill, or mixed domain) on the spatial domain for the asymptotic theory and the asymptotics purely come from the increasing time domain. We assume the space is fixed and bounded, and therefore both regularly and irregularly spaced spatial domain cases are covered here.

For $\mathbf{x} = (\mathbf{s}, t)^T$, $\mathbf{s} \in D \subset \mathbb{R}^d$, $t \in \mathbb{N}$, we assume that $Z(\mathbf{x})$ is a random field with mean zero. We consider the situation where the spatial domain for observations in D is fixed and the observations are taken regularly over time, $T_n = \{1, \dots, n\}$. We then divide D into two disjoint, nonempty subsets, D_1 and D_2 such that $D_1 \sqcup D_2 = D$. As in Section 2.1, we require the following assumptions on the random field, although we do not require the condition in (2) since the spatial locations are considered to be fixed. For the mixing condition, we define a mixing coefficient

$$\alpha(u) = \sup_{v \in \mathbb{N}} \left[\sup_{A, B} \{ |P(A \cap B) - P(A)P(B)|, A \in \mathcal{F}_{-\infty}^v, B \in \mathcal{F}_{v+u}^\infty \} \right], \quad (6)$$

where $\mathcal{F}_{-\infty}^v$ is the σ -algebra generated by the past time random field until $t = v$ and \mathcal{F}_{v+u}^∞ is the σ -algebra generated by the future time random field from time $t = v + u$. We use a slightly different version of mixing coefficient (6) from that in Li et al. (2008a,b), since we do not assume strong stationarity in time. Then we require the following strong mixing condition,

$$\alpha(u) = O(u^{-\epsilon}) \text{ for some } \epsilon > 0. \quad (7)$$

That is, we assume the random field is strongly mixing. Bradley (2005) discussed several mixing conditions, including strong mixing, for processes that are not necessarily stationary, provided examples of processes that satisfy certain mixing conditions, and described relationships between mixing conditions.

We consider a statistic (for $\mathbf{k} = (\mathbf{h}, u)$),

$$\hat{A}(\mathbf{k}; D) = \frac{1}{|S(\mathbf{h}; D)|(|T_n| - u)} \sum_{\mathbf{s} \in S(\mathbf{h}; D)} \sum_{t=1}^{n-u} Z(\mathbf{x})Z(\mathbf{x} + \mathbf{k}).$$

If Z is weakly stationary, the above statistic is an estimator of the covariance $C_0(\mathbf{k}) = \text{Cov}\{Z(\mathbf{x}), Z(\mathbf{x} + \mathbf{k})\}$. Let Λ be a set of space-time lags that we consider. We now establish the asymptotic joint normality of $\widehat{\mathbf{G}}_n = (\widehat{\mathbf{G}}_{n,1}, \widehat{\mathbf{G}}_{n,2})^T$ for $\widehat{\mathbf{G}}_{n,i} = \{\widehat{A}(\mathbf{k}; D_i) : \mathbf{k} \in \Lambda\}$. To do that we may require a few additional assumptions. The moment condition is that

$$\sup_n \mathbb{E}\{|\sqrt{|T_n|} |\widehat{A}(\mathbf{k}; D)|^{2+\delta}\} \leq C_\delta \text{ for some } \delta > 0, C_\delta < \infty. \quad (8)$$

To guarantee the existence and finiteness of the covariance matrix of $\widehat{\mathbf{G}}_n$, we may require the following condition ($\mathbf{x}_i = (\mathbf{s}_i, t_i)^T \in D \times T_n, i = 1, 2$)

$$\sum_{t_1=1}^{n-u_1} \sum_{t_2=1}^{n-u_2} \sum_{\mathbf{s}_1 \in S(\mathbf{h}_1; D_1)} \sum_{\mathbf{s}_2 \in S(\mathbf{h}_2; D_2)} \text{Cov}\{Z(\mathbf{x}_1)Z(\mathbf{x}_1 + \mathbf{k}_1), Z(\mathbf{x}_2)Z(\mathbf{x}_2 + \mathbf{k}_2)\} = O(n^2) \quad (9)$$

for all $\mathbf{k}_i = (\mathbf{h}_i, u_i)^T$ and \mathbf{h}_i, u_i finite ($i = 1, 2$).

Theorem 2. *Let $\{Z(\mathbf{x}) : \mathbf{x} \in \mathbb{R}^d \times \mathbb{N}\}$ be a spatio-temporal random field observed in $D \times T_n$, where $D \subset \mathbb{R}^d$ and $T_n = \{1, \dots, n\}$. If we consider two nonempty subsets D_1 and D_2 of D such that $D = D_1 \sqcup D_2$ and if we assume the condition in (9), then $\boldsymbol{\Sigma} = \lim_{n \rightarrow \infty} |T_n| \text{Var}(\widehat{\mathbf{G}}_n)$ exists and is finite. If we further assume that $\boldsymbol{\Sigma}$ is positive definite, that the conditions (7) and (8) hold, and that Z is weakly stationary with autocovariance function C_0 and if we let $\mathbf{G} = \{C_0(\mathbf{k}), \mathbf{k} \in \Lambda\}$, then $\sqrt{|T_n|}(\widehat{\mathbf{G}}_n - (\mathbf{G}, \mathbf{G})^T)$ is asymptotically normal with mean zero and covariance matrix $\boldsymbol{\Sigma}$.*

The above theorem is similar to Proposition 1 in Li et al. (2008b) except that Li et al. (2008b) required strong stationarity of the spatio-temporal random fields. The idea for the proof of Theorem 2 is similar to the proof of Theorem 1 given in the Appendix.

For the case that the spatial domain is spherical, unlike the case in Section 2.1, the asymptotic results simply follow from Theorem 2.

2.3 Extension to multivariate random fields

Recently covariance models for multivariate spatial or spatio-temporal random fields have received much attention and there are several papers that developed cross-covariance models for multivariate processes (e.g. Gneiting, Kleiber, and Schlather 2010; Apanasovich and Genton 2010; Apanasovich, Genton, and Sun 2011). The class of models developed in Jun (2009) gives non-stationary (axially symmetric) cross-covariances for multivariate processes on a sphere and the approach can easily be extended to spatio-temporal processes.

Consider a bivariate random field, $\mathbf{Z} = (Z_1, Z_2)^T$. Our goal here is to test whether the cross-covariance $\text{Cov}\{Z_1(\mathbf{x}_1), Z_2(\mathbf{x}_2)\}$ only depends on \mathbf{x}_1 and \mathbf{x}_2 through $\mathbf{x}_1 - \mathbf{x}_2$. Marginal weak stationarity of Z_1 and Z_2 does not necessarily imply weak stationarity of the cross-covariance structure of the two random fields. The basic idea of the asymptotic theory for the cross-covariance case is the same as in the univariate case and we simply need to modify the statistic \hat{A} in the following way (the spatio-temporal case is given as an example with $\mathbf{x} = (\mathbf{s}, t)$, $\mathbf{k} = (\mathbf{h}, u)$):

$$\hat{A}(\mathbf{k}; \cdot) = \frac{1}{|S(\mathbf{h}; \cdot)|(|T_n| - u)} \sum_{\mathbf{s} \in S(\mathbf{h}; \cdot)} \sum_{t=1}^{n-u} Z_1(\mathbf{x}) Z_2(\mathbf{x} + \mathbf{k}).$$

Here, we assume that the two random fields Z_1 and Z_2 are observed over the same spatial and temporal domains.

The asymptotic joint normality of $\hat{\mathbf{G}}_n$ holds for the spatial case under increasing domain asymptotics as in Section 2.1 and for the spatio-temporal case under increasing time domain asymptotics as in Sections 2.2. The idea of the proof is similar to the proof of the previous theorems. Similar results are presented in Li et al. (2008b), although their results are under the assumption that the multivariate process is strongly stationary.

3. TESTING PROCEDURE

3.1 Hypothesis and contrasts

We test the null hypothesis of weak stationarity of the random field. We may write this as $\hat{A}(\mathbf{k}; D_1) = \hat{A}(\mathbf{k}; D_2)$, where $\hat{A}(\cdot; D)$ is calculated from Z defined on D or $D \times T_n$ and $\mathbf{k} \in \Lambda$. Therefore we have $\mathbf{X}\hat{\mathbf{G}}_n = \mathbf{0}$ where \mathbf{X} is a full row rank matrix. In particular, for a spatial random field on \mathbb{R}^2 , if we consider $\Lambda = \{(1, 0), (0, 1)\}$, then we may let $\mathbf{X} = (\mathbf{I}_2, -\mathbf{I}_2)$, where \mathbf{I}_n denotes the identity matrix of dimension $n \times n$. Here, \mathbf{X} is of dimension 2×4 . Unlike the situations in Guan et al. (2004), Li et al. (2007, 2008a,b), and Li et al. (2009), we do not have ambiguity in choosing the contrast matrix \mathbf{X} . Once we choose the lags to use through Λ , the contrast matrix \mathbf{X} is automatically decided since \mathbf{X} should simply form the differences of \hat{A} values in two different spatial regions.

We give an example of how to construct a test statistic when we have spatio-temporal random fields. The test statistic for the spatial case works in the same way. Suppose we consider a spatio-temporal random field and $|\Lambda| = m$. Let $\mathcal{G} = \sqrt{|T_n|}(\hat{\mathbf{G}}_n - (\mathbf{G}, \mathbf{G})^T)$ using the same notation as in

Section 2.2. Define an $m \times 2m$ matrix \mathbf{X} such that $\mathbf{X} = (\mathbf{I}_m, -\mathbf{I}_m)$. Then our test statistic is given by

$$\mathcal{T}_m = (\mathbf{X}\mathcal{G})^T(\mathbf{X}\boldsymbol{\Sigma}\mathbf{X}^T)^{-1}\mathbf{X}\mathcal{G} \quad (10)$$

and due to Theorem 2, \mathcal{T}_m is asymptotically chi-square distributed with degrees of freedom m .

We estimate the covariance matrix, $\boldsymbol{\Sigma}$, using subsampling (Guan et al. 2004; Li et al. 2007, 2008a,b; Li et al. 2009). Similar L_2 -consistency of the subsampling estimator of the covariance matrix holds in our case due to (3), (4) and Theorem 1 in Ekström (2008). The results in Ekström (2008) do not require stationarity of the random field and assume a mixing condition weaker than (3). Therefore, if we replace $\boldsymbol{\Sigma}$ in (10) with $\hat{\boldsymbol{\Sigma}}$, the same asymptotic result holds by the multivariate Slutsky theorem, without additional conditions. As noted in Guan et al. (2004) for the spatial case (in Section 2.1) that the convergence of the asymptotic chi-square test statistic is slow, we explored both the asymptotic chi-square test and the calculation of p-values using subsampling. For the spatio-temporal case, we found that the convergence of the asymptotic chi-square test statistic was relatively fast.

3.2 Splitting the spatial domain

Our test statistic is based on the difference between estimators in two disjoint subsets of the spatial domain. In splitting the spatial domain, however, there is no one obvious way of doing it. Furthermore, two different collections of the random splitting sets may produce two different p-values and in some (but rare) situations the results of hypothesis testing may be different. Therefore, instead of splitting the domain into neighboring disjoint domains, it could be beneficial to randomly split the domain with respect to one of the spatial coordinates and repeat this procedure several times for both spatial coordinates. For example, Figure 2 gives an illustration of how to randomly split domains with respect to longitude or latitude for spherical data. This random splitting prevents us from getting spurious small p-values if it happens to be the case that there is a specific local spot where the values are either high or low (although the underlying random field is weakly stationary and the random field has mean zero).

In Section 2.1, we imposed a condition on the boundary of the spatial domain as in (2) for spatial processes. If we perform random splitting many times, there may be a case where the condition on the boundary of the spatial domain is not met. Thus, for this case, when we perform random

splitting, we have to keep in mind that we may need to avoid certain splits of the spatial domain, although the splits that may violate the condition in (2) are quite rare for a reasonably large n . When we do not have many spatial points to begin with, we have to ensure that there are enough pairs of spatial points in each splitted domain at the specified spatial lag. If the spatial domain is not regularly spaced, we may overlay a regular grid over the spatial domain and split the domain based on that grid.

It is not clear what the distribution of the collection of p-values from random splitting should be since the test statistics from different random splitting are not independent. Figure 3 displays the histograms and boxplots of the p-values from 130 random splits with respect to longitude and latitude for 1000 simulations from the weakly stationary random field in Section 4.2. Although the histograms show that there are peaks near the boundaries in the distribution of p-values, the distribution is close to be uniform away from the end points. We cannot make a direct comparison between the boxplots in Figure 3 and those figures of p-values in Section 5 since the underlying covariance structure may be different. Nonetheless, we have a general idea on how the distribution of p-values should look like under weak stationarity from Figure 3.

We may also consider splitting into more than two spatial domains although if we split too much we may not have enough sample size in each sub-domain to get reliable \widehat{A} values. Therefore, we fix the number of subdomains to be two for each split throughout the paper.

3.3 Choice of lags

Under our test setting, we may choose particular sets of spatial or temporal lags depending on what we want to test. For example, if we consider a spatio-temporal random field on a sphere, and if we want to test whether the random field is axially symmetric and stationary in time, we may choose a set of lags that only involves lags with respect to longitude and time. Similarly if we want to test if the random field is nonstationary with respect to latitude or not, we may choose a set of lags that only involves latitude. Although the distance on the globe depends on the two latitude points, if the longitudinal lag is zero, then the distance only depends on the latitudinal lag. Therefore, with the lags that only involve latitude, we can test if the random field is actually nonstationary in latitude or not.

We acknowledge, however, that similarly to the tests proposed in Guan et al. (2004) and Li et al. (2008a,b), the conclusion from our test on stationarity only holds for the particular lags that we

consider. Even if we conclude from our test that the random field is stationary, the random field might still be nonstationary for some pairs of locations (and time points) with lags not considered in the particular test set.

4. SIMULATION STUDIES

4.1 Spatial random field on a regularly spaced planar domain

We consider a mean zero weakly stationary (isotropic) Gaussian random field $Z(\mathbf{s})$, $\mathbf{s} \in D \subset \mathbb{Z}^2$ and we assess the size of the test. Then we calculate the power of the test based on some nonstationary covariance models. The covariance/correlation structure that we use to assess the size of the test is given by

$$C_0(\mathbf{h}; m) = \begin{cases} 1 - \frac{3\|\mathbf{h}\|}{m} + \frac{\|\mathbf{h}\|^3}{2m^3} & \text{if } 0 \leq \|\mathbf{h}\| \leq m, \\ 0 & \text{otherwise,} \end{cases} \quad (11)$$

where m defines the range and strength of dependence. We test the cases $m = 2, 5, 8$. We generate 1000 realizations for each m on 40×20 or 80×40 rectangular grids. For the test statistic, we split the domain into two 20×20 or 40×40 neighboring squares (thus we do not perform the random splitting discussed in Section 3.2). Therefore, the statistic \hat{A} is calculated on two of the 20×20 or 40×40 square domains. We use the following sets:

$$\Lambda_1 = \{\mathbf{h} : (1, 0), (0, 1)\},$$

$$\Lambda_2 = \{\mathbf{h} : (1, 0), (0, 1), (1, 1), (-1, 1)\},$$

$$\Lambda_3 = \{\mathbf{h} : (1, 0), (0, 1), (1, 1), (-1, 1), (2, 1), (1, 2), (-2, 1), (-1, 2)\}.$$

We explore both the asymptotic chi-squared test and the subsampling approach to compute the p-values, and we use subsampling to estimate Σ . We also applied the same finite-sample adjustments as in Guan et al. (2004). Table 1 gives the empirical sizes based on p-values using subsampling. We do not report the outcomes from the asymptotic chi-squared test since the convergence of the test statistic is rather slow due to the small sample size n , but the results are qualitatively similar.

For the empirical power, we use the nonstationary model in Paciorek and Schervish (2006). If D is the regular grid of size $2n \times n$ ($n = 20$ or 40) and if $\mathbf{s}_1, \mathbf{s}_2 \in D$, we consider a nonstationary

covariance function in the following form:

$$C(\mathbf{s}_1, \mathbf{s}_2) = |\boldsymbol{\Sigma}_1|^{1/4} |\boldsymbol{\Sigma}_2|^{1/4} \left| \frac{\boldsymbol{\Sigma}_1 + \boldsymbol{\Sigma}_2}{2} \right|^{-1/2} \exp(\sqrt{Q_{12}}), \quad (12)$$

with $Q_{12} = 2(\mathbf{s}_1 - \mathbf{s}_2)^T (\boldsymbol{\Sigma}_1 + \boldsymbol{\Sigma}_2)^{-1} (\mathbf{s}_1 - \mathbf{s}_2)$. We decompose $\boldsymbol{\Sigma}_i = \boldsymbol{\Gamma}_i \boldsymbol{\Lambda}_i \boldsymbol{\Gamma}_i^T$ for $i = 1, 2$, where

$$\boldsymbol{\Gamma}_i = \frac{1}{d_i} \begin{pmatrix} \gamma_1(\mathbf{s}_i) & -\gamma_2(\mathbf{s}_i) \\ \gamma_2(\mathbf{s}_i) & \gamma_1(\mathbf{s}_i) \end{pmatrix}, \quad \boldsymbol{\Lambda}_i = \begin{pmatrix} d_i^2 & 0 \\ 0 & \frac{d_i^2}{2} \end{pmatrix},$$

$d_i = \sqrt{\gamma_1^2(\mathbf{s}_i) + \gamma_2^2(\mathbf{s}_i)}$, $\gamma_1(\mathbf{s}) = \log\{s_x/(2n)\}$, $\gamma_2(\mathbf{s}) = \{s_x/(2n)\}^2 + \{s_y/n\}^2$, and $\mathbf{s} = (s_x, s_y)^T$. The forms of γ_1 and γ_2 are chosen arbitrarily to create a smooth nonstationary covariance structure through (12) (see Figure 4). Porcu, Mateu, and Christakos (2009) gave a more general framework for the nonstationary covariance models which includes the model in (12). In (12), we do not use the covariance function in (11) since the scale of $\sqrt{Q_{12}}$ is not comparable to the original distances between \mathbf{s}_1 and \mathbf{s}_2 . Although the exponential covariance function does not have a compact support, we find that many of the covariance values calculated from (12) are close to zero in our domain and the effective length of the support is small.

Table 1 gives the empirical size values of the test from subsampling when the nominal value is 5%. There is no clear association between the size values and the number of lags chosen. Overall the empirical sizes of the test are close to the nominal value, although the empirical sizes are somewhat large for small numbers of lags or when the dependence of the simulated process is strong ($m = 8$). The empirical sizes are closer to the nominal value when the sample size n is larger. The empirical powers using the nonstationary model in (12) from subsampling are given in Table 2. The empirical power values are significantly bigger for $n = 40$, which we expect. There is no clear association between the empirical power and the number of lags chosen. For $n = 40$, it seems that the empirical powers decrease as we use larger subblock lengths for each number of lags, although it is not the case when $n = 20$.

4.2 Spatio-temporal random field on a spherical domain

We consider a regularly spaced grid on the surface of a sphere and regularly spaced time points. This set up is common for global spatio-temporal data (for example, see Section 5.2). We simulate a random field from a first-order vector autoregressive model, VAR(1), $\mathbf{Z}_t = \mathbf{R} \mathbf{Z}_{t-1} + \boldsymbol{\epsilon}_t$, where $\mathbf{Z}_t = \{Z(\mathbf{s}_1, t), \dots, Z(\mathbf{s}_k, t)\}^T$, $\mathbf{s}_i \in D$, $i = 1, \dots, k$, $t = 1, \dots, T$. Here k is the number of observed

points in the spatial domain D and T is the number of time points. We assume that ϵ_t is a mean zero Gaussian multivariate random field on a sphere with a spatially isotropic exponential correlation function and ϵ_t is independent across time. The matrix \mathbf{R} gives the autoregressive coefficients.

Figure 5 shows the spatial locations of points at which we simulate the data. We have 11 regularly spaced latitude points from 50° S to 40° N and 11 regularly spaced longitude points from 0° to 180° . For the spatial covariance function, we use an isotropic function, $C_0(\mathbf{h}) = \exp(-\frac{\|\mathbf{h}\|}{1000})$ and for the temporal correlation, we use $\mathbf{R} = 0.4 \times \mathbf{I}_k$. The spatial distance used is chordal distance on the surface of a sphere and \mathbf{I}_k is the identity matrix. Here $k = 11^2 = 121$ and $T = 400$. We estimate Σ using a subsampling technique. As described in Section 3.2, we try random splitting of the domain with respect to latitude as well as with respect to longitude. We created 130 random splits for each splitting with respect to latitude and longitude. There are at most $\binom{11}{5} = 462$ ways of splitting the domain randomly into two disjoint domains and quite a few of them only contain pairs of spatial points with spatial lag greater than 1.

The assessment of the power of the test is done under the situation that the random field is nonstationary with respect to latitude but stationary in longitude and time (that is, the random field is axially symmetric and stationary in time). We simulated an axially symmetric random field (time structure is still AR(1)) using the covariance function in Jun and Stein (2008). In particular, for a latitude point L and a longitude point l , we set

$$Z(L, l, 0) = \left\{ A(L) \frac{\partial}{\partial L} + B(L) \frac{\partial}{\partial l} \right\} W(L, l) \quad (13)$$

with $A(L) = 1 + 0.5P_1(\sin L) + P_2(\sin L) - 0.5P_3(\sin L)$ and $B(L) = 1 - 2P_1(\sin L) - P_2(\sin L) + 0.05P_3(\sin L)$, where P_n is the Legendre polynomial of degree n . The coefficients in the linear combinations for A and B are chosen arbitrarily. The random field W is a mean zero Gaussian random field with the covariance structure given by a Matérn covariance function,

$$\text{Cov}\{W(L_1, l_1), W(L_2, l_2)\} = (d/1000)^{1.5} \mathcal{K}_{1.5}(d/1000),$$

where d is the chordal distance between the two points, (L_1, l_1) and (L_2, l_2) , and \mathcal{K}_ν denotes the modified Bessel function of order ν . As discussed in Jun and Stein (2008), the model in (13) is axially symmetric but nonstationary with respect to latitude.

We use the following sets of lags:

$$\Lambda_1 = \{(L, l, u) : (1, 0, 0), (2, 0, 0)\},$$

$$\Lambda_2 = \{(L, l, u) : (0, 1, 1), (0, 2, 1), (0, 1, 2), (0, 2, 2)\}.$$

In the above lags, the unit of the latitude is 10° and that of the longitude is 18° . The first set of lags, Λ_1 , is to check the stationarity with respect to latitude and Λ_2 is to check stationarity in longitude and time. The size of subblocks used here is 5, 10, and 20.

Table 3 shows the empirical size and power for each split. It is interesting to note that when we split the domain with respect to longitude, we cannot detect nonstationarity with respect to latitude. This is what we expect since if the random field is nonstationary with respect to latitude but stationary with respect to longitude and if we split with respect to longitude, the expected difference of the estimators between the two splitted spatial domains should be zero. Therefore we should not see any difference in the empirical size and powers (except random variation) and both quantities should be close to the nominal level. However, when we split the domain with respect to latitude, we do detect nonstationarity with respect to latitude as we expect.

5. APPLICATIONS

5.1 Pacific Ocean wind data

We consider the Pacific Ocean wind data that was studied by Wikle and Cressie (1999), Cressie and Huang (1999), Guan et al. (2004), and Li et al. (2007). The data consist of the East-West component of the wind velocity vector from a small region over the tropical western Pacific Ocean for the period from November 1992 to February 1993. The time resolution is 6 hours and there are a total 480 time points. The spatial domain is a regularly spaced 17×17 grid with 1.875° (lon) by 1.9047° (lat) resolution. Wikle and Cressie (1999) considered spatial isotropic covariance models and Cressie and Huang (1999) fitted space-time stationary covariance models to these data. Guan et al. (2004) found some evidence against isotropy for this data set. In particular, they found that the variogram for the North-South direction is not bounded when the lag distance gets larger, which may suggest nonstationarity with respect to latitude.

We test the stationarity assumption in the space and time domains using our procedure. The test is based on an asymptotic chi-squared distribution assuming the time length $T = 480$ is large enough. Before we perform the hypothesis test, we need to remove the fixed mean part of the data

so that the residuals are close to be mean zero. Wikle and Cressie (1999) and Li et al. (2007) removed the temporal average of the data (average over time at each grid pixel) while Cressie and Huang (1999) and Guan et al. (2004) did not explain if any procedure was done to make the process close to be mean zero before their analysis. The results in Cressie and Huang (1999) indicate that they used the raw data without removing the mean part. In our preliminary result of the data analysis, however, there seems to be a persistent spatial pattern in the data over time and certainly removing temporal average should help to get rid of some of these patterns (the pattern shown in Figure 6 (a)). We also found that even after removing temporal average from the data, there is still a non-negligible trend in the data (see Figure 6 (b)). As for the tests in Guan et al. (2004) and Li et al. (2007), our test assumes that the spatio-temporal field is mean zero. Therefore, how we take care of the fixed mean structure of the data certainly has some impact on the results of the test. To see the effect of the fixed mean part, we performed the test on the raw data (after removing the grand mean), on the data with only temporal average removed, on the data with only spatial average removed, and on the data with both spatial and temporal averages removed.

We consider several combinations of space-time lags for the test. We use

$$\begin{aligned}\Lambda_1 &= \{(L, l, u) : (1, 0, 0), (2, 0, 0)\}, \\ \Lambda_2 &= \{(L, l, u) : (0, 1, 0), (0, 2, 0)\}, \\ \Lambda_3 &= \{(L, l, u) : (1, 0, 0), (0, 1, 0), (1, 1, 0)\}, \\ \Lambda_4 &= \{(L, l, u) : (1, 0, 1), (0, 1, 1), (1, 1, 1)\}.\end{aligned}$$

In the above sets, the unit for the lag with respect to longitude is 1.875° and the one with respect to latitude is 1.9047° . The set Λ_1 is to test stationarity with respect to latitude, Λ_2 for longitude, Λ_3 for space, and Λ_4 for space and time together. We tried various sizes of subblocks and random splitting of the domain, some with respect to latitude and some with respect to longitude. For both cases of splitting with respect to latitude and longitude, we performed 1000 random splitting as described in Section 3.2.

Figure 7 shows the p-values from the test. First notice that the test results on raw data and the data with spatial and temporal averages removed give large p-values for Λ_1 when we split the domain with respect to longitude, while p-values are small for the same lags when the split is with respect to latitude. This is a clear sign that for both data, the nonstationarity with respect to latitude is significant. We saw a similar phenomenon in the simulated data (Table 3). On the other

hand, the p-values for Λ_2 , Λ_3 , and Λ_4 for the split with respect to longitude are quite different for the two data sets. We suspect that the reason why we get small p-values for Λ_2 , Λ_3 , and Λ_4 for the raw data is that the spatial pattern in the temporal average (shown in Figure 6 (a)) has a significant effect on the test statistics and thus we get quite large test statistics. Therefore, we conclude that it is necessary to remove both spatial and temporal averages from the data. We also checked that the p-values for the data with only temporal average removed and those for the data with spatial and temporal averages removed are quite similar (not shown). The p-values for Λ_2 for the data with spatial and temporal averages removed are quite large for both splitting schemes. This supports the argument that the random field is indeed axially symmetric.

5.2 Global surface temperature data

We analyze monthly global surface temperature data over 50 years. In particular, we use observations of the combined data set of the land and the ocean from the Climate Research Unit, East Anglia and the Hadley Centre. The climate model outputs used in this paper are from the NOAA GFDL model (GFDL-CM2.0). Jun, Knutti, and Nychka (2008) modeled the difference between observations and climate model outputs as climate model errors (we call this “diff” from now on) and used a simple nonstationary covariance model. They only considered a spatial component and their model is isotropic in space except that the covariance is larger over the land than over the ocean. Here we test the axial symmetry (and stationarity in time) as well as nonstationarity with respect to latitude using the methodology developed in this paper.

Even though we remove the fixed mean part using the observations as an effective mean, we may still have some non-negligible mean part due to the complex error structure of the climate models. In particular, it turns out that the “diff” random field has non-negligible seasonality in many grid pixels. Figure 8 shows the periodogram of the “diff” time series at the grid pixel with latitude 47.5° S and longitude 47.5° E. The figure is generated using an R function, *spec.pgram*. Notice the peaks at several frequencies which correspond to an annual cycle and cycles of a few years length. Therefore, we use least squares with sine and cosine curves for the frequency of one year up to six years to remove the seasonality in the trend. After this step, we do not see any noticeable mean structure.

The lags used for the test are the following:

$$\begin{aligned}\Lambda_1 &= \{(L, l, u) : (1, 0, 0)\}, \\ \Lambda_2 &= \{(L, l, u) : (1, 0, 0), (2, 0, 0)\}, \\ \Lambda_3 &= \{(L, l, u) : (0, 1, 1), (0, 1, 2)\}, \\ \Lambda_4 &= \{(L, l, u) : (0, 1, 1), (0, 1, 2), (0, 2, 1), (0, 2, 2)\}.\end{aligned}$$

Thus, Λ_1 and Λ_2 are to test for stationarity with respect to latitude and Λ_3 and Λ_4 are for stationarity with respect to longitude and time. We perform random splitting 1000 times with respect to longitude as well as an additional 1000 times with respect to latitude. Figure 9 gives the p-values for each split. First notice that p-values for Λ_3 and Λ_4 are quite large when the split is with respect to longitude while they are quite small when the split is with respect to latitude (notice the scale difference of the y-axis for the two figures). In fact, the p-values for Λ_3 when the split is done with respect to longitude seem to have a similar distribution as the one in Figure 3. This is a clear sign that the random field is axially symmetric. The p-values for Λ_1 and Λ_2 for both ways of split are close to zero, which is an indication that the random field is strongly nonstationary with respect to latitude. Therefore, we conclude that even if we model the difference between the observations and the climate model outputs, nonstationarity is significant with respect to latitude in the difference random field. Hence the axially symmetric models that are nonstationary with respect to latitude in Jun and Stein (2007, 2008) seem appropriate for modeling the difference random fields.

6. DISCUSSION

In the proposed test, both Theorem 1 and Theorem 2 require the covariance matrices $\hat{\Sigma}$, $\hat{\Sigma}_{11}$, and $\hat{\Sigma}_{22}$ to be positive definite. In our simulation studies and the real data applications, we checked the eigenvalues of the estimates of these matrices for all lags considered and all subblock sizes used and we found that all the eigenvalues were positive.

We do not make the assumption that the random field is Gaussian. If the random field under consideration is Gaussian, then weak stationary under the null hypothesis implies strong stationarity. Therefore the asymptotic results in Guan et al. (2004) and Li et al. (2007, 2008a,b) that require strong stationarity can be applied directly for our situation. Particularly, (5), (6), and (9) can be simplified as in Guan et al. (2004) and Li et al. (2007, 2008a,b). However we still need to show the joint asymptotic normality of $\hat{\mathbf{G}}_{n,1}$ and $\hat{\mathbf{G}}_{n,2}$ as in A.2 of the Appendix.

One issue in performing our test is how to determine the subblock size. For a spatio-temporal random field, if the temporal structure of the random field is AR(1), we may use the subblock of size $l(n) = (\frac{2\gamma}{1-\gamma^2})^{2/3}(\frac{3n}{2})^{1/3}$ where n is the length of time points and γ is the estimate of the AR(1) coefficient (as noted in Li et al. 2007). For more general random fields, we can resort to model free approaches such as those in Lahiri (2003). Alternatively, we may use similar ideas as in Shao and Li (2009) who used inconsistent estimators to normalize out the asymptotic covariance matrix and are free of the parameter for the subblock size. Although this direction could be worthwhile to pursue, it may suffer from loss of power.

In reality, many data sets do not come from a stationary process. However, common practice is to fit stationary (in fact, isotropic) models to real data sets without thoroughly checking the assumptions. In fact there are only a limited number of nonstationary covariance models developed so far. On the other hand, many global data sets exhibit stationarity with respect to longitude and time in the covariance structure, although they have strong nonstationarity with respect to latitude. Our motivation is to provide a formal statistical testing procedure of the stationarity assumption, in particular, the axial symmetry assumption (i.e. process being stationary with respect to longitude) and the stationarity assumption in time. If we fail to reject the latter, we would recommend using the stationary models to fit the data. If we do reject the stationarity assumption, we need to develop a nonstationary model that can properly describe the nonstationarity in the data.

Even if we reject the null hypothesis in our test, it is possible that the process is still weakly stationary but some of the moment or mixing conditions required for the asymptotic normality may not hold. This type of problem is common in the test based on asymptotic results and similar problems exist in the tests proposed in Guan et al. (2004) and Li et al. (2007, 2008a,b). At least for the data sets considered in the application of this paper, we think the moment and mixing conditions required for Theorem 2 are reasonable.

There may be situations where our test has little power in detecting nonstationarity in space. For example, if the nonstationarity varies slowly for short distances in space, we may not detect such nonstationarity well with the random splitting described in Section 3.2. On the other hand, if we are only interested in testing stationarity in time of a spatio-temporal random field, in some situations, especially for a random field that does not induce space-time interactions in the covariance structure (i.e. spatio-temporal separable), the proposed test may not detect nonstationarity in time. For this situation, we may need to split the temporal domain as we split the spatial domain, to detect

nonstationarity in time and may need to adjust the theory accordingly. However, the focus of the work presented in this paper was to test stationarity in space or axial symmetry, not to test temporal stationarity alone.

APPENDIX: Proof of Theorems

Proof of Theorem 1

We first show that the asymptotic normality of $\sqrt{|D_{n,i}|}(\widehat{\mathbf{G}}_{n,i} - \mathbf{G})^T$ for each i holds under the conditions given in Section 2.1. Then we show the joint asymptotic normality of $(\sqrt{|D_{n,1}|}(\widehat{\mathbf{G}}_{n,1} - \mathbf{G}), \sqrt{|D_{n,2}|}(\widehat{\mathbf{G}}_{n,2} - \mathbf{G}))^T$.

A.1 Asymptotic normality of $\sqrt{|D_{n,1}|}(\widehat{\mathbf{G}}_{n,1} - \mathbf{G})^T$: If the condition (5) holds, then the existence of the limit of the covariance of $\widehat{\mathbf{G}}_{n,1}$ is trivial. For a lag $\mathbf{h} \in \Lambda$, we let $\sigma_1^2 = \lim_{n \rightarrow \infty} |D_{n,1}| \text{Cov}\{\widehat{\mathbf{G}}_{n,1}(\mathbf{h}) - \mathbf{G}(\mathbf{h}), \widehat{\mathbf{G}}_{n,1}(\mathbf{h}) - \mathbf{G}(\mathbf{h})\}$.

Let $S_{n,1} \equiv \sqrt{|D_{n,1}|}(\widehat{\mathbf{G}}_{n,1}(\mathbf{h}) - \mathbf{G}(\mathbf{h}))$. We show $S_{n,1} \xrightarrow{d} N(0, \sigma_1^2)$. Let $l(n) = n^\alpha$, $m(n) = n^\alpha - n^\eta$ for some $\frac{4}{2+\epsilon} < \eta < \alpha < 1$. Divide $D_{n,1}$ into nonoverlapping $l(n) \times l(n)$ subsquares, $D_{l(n),1}^j$, $j = 1, \dots, k_n$. Within each subsquare, we further get $D_{m(n),1}^j$, which shares the same center as $D_{l(n),1}^j$. Therefore we have $d(D_{m(n),1}^j, D_{m(n),1}^{j'}) \geq n^\eta$, $j \neq j'$. Now for a particular lag \mathbf{h} that we consider, let $\widehat{\mathbf{G}}_{m(n),1}^j(\mathbf{h})$ denote the statistic obtained from $D_{m(n),1}^j$. Let $s_{n,1} = \sum_{j=1}^{k_n} s_{n,1}^j / \sqrt{k_n}$ and $s'_{n,1} = \sum_{j=1}^{k_n} (s_{n,1}^j)' / \sqrt{k_n}$, where $s_{n,1}^j = m(n)\{\widehat{\mathbf{G}}_{m(n),1}^j(\mathbf{h}) - \mathbf{G}(\mathbf{h})\}$ and $(s_{n,1}^j)'$ have the same marginal distribution as $s_{n,1}^j$ but are independent.

We now let $\phi_{n,1}(x)$ and $\phi'_{n,1}(x)$ be the characteristic functions of $s_{n,1}$ and $s'_{n,1}$, respectively. We follow the three steps given below to complete the proof:

- S1. $S_{n,1} - s_{n,1} \xrightarrow{p} 0$;
- S2. $\phi'_{n,1}(x) - \phi_{n,1}(x) \rightarrow 0$;
- S3. $s'_{n,1} \xrightarrow{d} N(0, \sigma_1^2)$.

Proof of S1. It suffices to show $E(S_{n,1} - s_{n,1})^2 \rightarrow 0$ as $n \rightarrow \infty$. Let $D_1^{m(n)}$ denote the union of all $D_{m(n),1}^j$. Simple algebra shows that $s_{n,1}$ can be written as $\sqrt{|D_1^{m(n)}|}\{\widehat{\mathbf{G}}_{D_1^{m(n)}}(\mathbf{h}) - \mathbf{G}(\mathbf{h})\}$. Given the condition in (2), it can be shown that $|D_1^{m(n)}|/|D_{n,1}| \rightarrow 1$. Then using the moment condition in (5), we get $E(S_{n,1} - s_{n,1})^2 \rightarrow 0$ as $n \rightarrow \infty$.

Proof of S2. Let ι denote the imaginary number. We set $U_i = \exp(\iota x \frac{s_{n,1}^i}{\sqrt{k_n}})$, $X_k = \prod_{i=1}^k U_i$, and $Y_k = U_{k+1}$. Due to Lemma A.2 (b) of Ekström (2008), we have $|\text{Cov}(X_k, Y_k)| \leq c \cdot \alpha(n^2, n^\eta)$ for some constant $c > 0$. We now apply a similar telescope argument as in p.338 of Ibragimov and Linnik (1971) in the following way. Suppose the characteristic function of $\frac{s_{n,1}^i}{\sqrt{k_n}}$ is given by $\phi_{n,1}^{(i)}$ (since we do not assume strong stationarity, $\frac{s_{n,1}^i}{\sqrt{k_n}}$ may not have the same distribution). Then

$$\begin{aligned}
|\phi_{n,1}(x) - \prod_{i=1}^{k_n} \phi_{n,1}^{(i)}(x)| &= |E(X_{k_n}) - \prod_{i=1}^{k_n} \phi_{n,1}^{(i)}(x)| \\
&= |E(X_{k_n}) - \phi_{n,1}^{(k_n)}(x)E(X_{k_n-1}) + \phi_{n,1}^{(k_n)}(x)E(X_{k_n-1}) - \prod_{i=1}^{k_n} \phi_{n,1}^{(i)}(x)| \\
&\leq |E(X_{k_n}) - \phi_{n,1}^{(k_n)}(x)E(X_{k_n-1})| + |E(X_{k_n-1}) - \prod_{i=1}^{k_n-1} \phi_{n,1}^{(i)}(x)| \\
&= |\text{Cov}(X_{k_n-1}, Y_{k_n-1})| + |E(X_{k_n-1}) - \prod_{i=1}^{k_n-1} \phi_{n,1}^{(i)}(x)| \\
&\leq c \cdot \alpha(n^2, n^\eta) + |E(X_{k_n-1}) - \prod_{i=1}^{k_n-1} \phi_{n,1}^{(i)}(x)| \\
&\leq \dots \leq k_n \cdot c \cdot \alpha(n^2, n^\eta) \rightarrow 0 \text{ as } n \rightarrow 0.
\end{aligned} \tag{14}$$

Note that (14) holds due to (3). Since $(s_{n,1}^i)'$ have the same marginal distribution as $s_{n,1}^i$ but are independent, (14) implies $|\phi_{n,1}(x) - \phi'_{n,1}(x)| \rightarrow 0$ as $n \rightarrow 0$.

Proof of S3. This follows from the Lyapounov theorem.

Proof of the joint normality. The joint normality of the vector across several spatial lags can be shown using the Cramér-Wold device.

A.2 Joint asymptotic normality of $(\sqrt{|D_{n,1}|}(\widehat{\mathbf{G}}_{n,1} - \mathbf{G}), \sqrt{|D_{n,2}|}(\widehat{\mathbf{G}}_{n,2} - \mathbf{G}))^T$: The basic idea of the proof is similar to the one in A.1. If the condition (5) holds, then the existence of the limit of the covariance between $\widehat{\mathbf{G}}_{n,i}$ and $\widehat{\mathbf{G}}_{n,j}$ ($i, j = 1, 2$) is trivial. For a lag $\mathbf{h} \in \Lambda$, we let $\sigma_i^2 = \lim_{n \rightarrow \infty} |D_{n,i}| \text{Var}\{\widehat{\mathbf{G}}_{n,i}(\mathbf{h}) - \mathbf{G}(\mathbf{h})\}$ for $i = 1, 2$ and $\sigma_{ij} = \lim_{n \rightarrow \infty} \sqrt{|D_{n,i}| |D_{n,j}|} \text{Cov}\{\widehat{\mathbf{G}}_{n,i}(\mathbf{h}) - \mathbf{G}(\mathbf{h}), \widehat{\mathbf{G}}_{n,j}(\mathbf{h}) - \mathbf{G}(\mathbf{h})\}$ for $i \neq j$.

Let a and b be two arbitrary real numbers such that $|a| \leq 1$, $|b| \leq 1$ and at least one of them is not zero. Now we set

$$S_n = a\sqrt{|D_{n,1}|}\{\widehat{\mathbf{G}}_{n,1}(\mathbf{h}) - \mathbf{G}(\mathbf{h})\} + b\sqrt{|D_{n,2}|}\{\widehat{\mathbf{G}}_{n,2}(\mathbf{h}) - \mathbf{G}(\mathbf{h})\} \equiv aS_{n,1}(\mathbf{h}) + bS_{n,2}(\mathbf{h}).$$

Also let $s_n = as_{n,1}(\mathbf{h}) + bs_{n,2}(\mathbf{h})$ and $s'_n = as'_{n,1}(\mathbf{h}) + bs'_{n,2}(\mathbf{h})$. We further assume that $(s_{n,1}^j, s_{n,2}^j)$ and $((s_{n,1}^j)', (s_{n,2}^j)')$ have the same distribution for each j and $(s_{n,1}^j)'$ and $(s_{n,2}^j)'$ are independent for each j . Moreover, we assume $(s_{n,1}^j)'$ and $(s_{n,2}^{j'})'$ are independent for $j \neq j'$.

We now let $\phi_n(x)$ and $\phi'_n(x)$ be the characteristic functions of s_n and s'_n , respectively. We follow the three steps given below to complete the proof:

S4. $S_n - s_n \xrightarrow{p} 0$;

S5. $\phi'_n(x) - \phi_n(x) \rightarrow 0$;

S6. $s'_n \xrightarrow{d} N(0, \sigma^2)$ with $\sigma^2 = a^2\sigma_1^2 + b^2\sigma_2^2 + 2ab\sigma_{12}$.

Proof of S4. Due to the result in S1, it is trivial to show $S_n - s_n \xrightarrow{p} 0$.

Proof of S5. Due to the result in S2 and a similar telescope argument, we can show that

$$|\phi'_n(x) - \phi_n(x)| \rightarrow 0 \text{ as } n \rightarrow 0.$$

Proof of S6. This again follows from the Lyapounov theorem.

Proof of the joint normality. This also follows from the Cramér-Wold device.

□

REFERENCES

- Apanasovich, T. V. and Genton, M. G. (2010), “Cross-covariance functions for multivariate random fields based on latent dimensions,” *Biometrika*, 97, 15–30.
- Apanasovich, T. V., Genton, M. G., and Sun, Y. (2011), “A valid Matérn class of cross-covariance functions for multivariate random fields with any number of components,” IAMCS preprint series 2011-204, Texas A&M University.
- Bevilacqua, M., Mateu, J., Porcu, E., Zhang, H., and Zini, A. (2010), “Weighted composite likelihood-based tests for space-time separability of covariance functions,” *Statistics and Computing*, 20, 283–293.
- Bradley, R. C. (2005), “Basic properties of strong mixing conditions. A survey and some open questions,” *Probability Surveys*, 2, 107–144.
- Cressie, N. and Huang, H. C. (1999), “Classes of nonseparable, spatio-temporal stationary covariance functions,” *Journal of the American Statistical Association*, 94, 1330–1340.
- Dwivedi, Y. and Subba Rao, S. (2010), “A test for second order stationarity of a time series based on the Discrete Fourier Transform,” *Journal of Time Series Analysis*, 32, 68–91.
- Ekström, M. (2008), “Subsampling variance estimation for non-stationary spatial lattice data,” *Scandinavian Journal of Statistics*, 35, 38–63.
- Fuentes, M. (2005), “A formal test for nonstationarity of spatial stochastic processes,” *Journal of Multivariate Analysis*, 96, 30–55.
- (2006), “Testing for separability of spatial-temporal covariance functions,” *Journal of Statistical Planning and Inference*, 136, 447–466.
- Gneiting, T., Genton, M. G., and Guttorp, P. (2007), *Geostatistical space-time models, stationarity, separability and full symmetry*, pp. 151–175, Monographs in Statistics and Applied Probability, Chapman & Hall/CRC Press.
- Gneiting, T., Kleiber, W., and Schlather, M. (2010), “Matérn cross-covariance functions for multivariate random fields,” *Journal of the American Statistical Association*, 105, 1167–1177.

- Guan, Y., Sherman, M., and Calvin, J. A. (2004), “A nonparametric test for spatial isotropy using subsampling,” *Journal of the American Statistical Association*, 99, 810–821.
- Ibragimov, I. and Linnik, Y. (1971), *Independent and Stationary Sequences of Random Variables*: Wolters-Noordhoff Publishing.
- Jones, R. H. (1963), “Stochastic processes on a sphere,” *The Annals of Mathematical Statistics*, 34, 213–218.
- Jun, M. (2009), “Nonstationary cross-covariance models for multivariate processes on a globe,” Technical Report 2009-110, IAMCS preprint series.
- Jun, M., Knutti, R., and Nychka, D. W. (2008), “Spatial analysis to quantify numerical model bias and dependence: How many climate models are there?” *Journal of the American Statistical Association*, 103, 934–947.
- Jun, M. and Stein, M. L. (2007), “An approach to producing space-time covariance functions on spheres,” *Technometrics*, 49, 468–479.
- (2008), “Nonstationary covariance models for global data,” *Annals of Applied Statistics*, 2, 1271–1289.
- Lahiri, S. N. (1996), “On inconsistency of estimators based on spatial data under infill asymptotics,” *Shankya: The Indian Journal of Statistics, Series A*, 58, 403–417.
- (2003), *Resampling Methods for Dependent Data*, New York: Springer-Verlag.
- Li, B., Genton, M. G., and Sherman, M. (2007), “A nonparametric assessment of properties of space-time covariance functions,” *Journal of the American Statistical Association*, 102, 736–744.
- (2008a), “On the asymptotic joint distribution of sample space-time covariance estimators,” *Bernoulli*, 14, 228–248.
- (2008b), “Testing the covariance structure of multivariate random fields,” *Biometrika*, 95, 813–829.

- Li, B., Murthi, A., Bowman, K. P., North, G. R., Genton, M. G., and Serman, M. (2009), “Statistical tests of Taylor’s hypothesis: An application to precipitation fields,” *Journal of Hydrometeorology*, 10, 254–265.
- Mitchell, M., Genton, M. G., and Gumpertz, M. (2005), “Testing for separability of space-time covariances,” *Environmetrics*, 16, 819–831.
- (2006), “A likelihood ratio test for separability of covariances,” *Journal of Multivariate Analysis*, 97, 1025–1043.
- Paciorek, C. J. and Schervish, M. J. (2006), “Spatial modelling using a new class of nonstationary covariance functions,” *Environmetrics*, 17, 483–506.
- Porcu, E., Mateu, J., and Christakos, G. (2009), “Quasi-arithmetic means of covariance functions with potential applications to space-time data,” *Journal of Multivariate Analysis*, 100, 1830–1844.
- Priestley, M. B. and Subba Rao, T. (1969), “A test for stationarity of time series,” *Journal of the Royal Statistical Society, Series B*, 31, 140–149.
- Shao, X. and Li, B. (2009), “A tuning parameter free test for properties of space-time covariance functions,” *Journal of Statistical Planning and Inference*, 139, 4031–4038.
- Stein, M. L. (1995), “Fixed domain asymptotics for spatial periodograms,” *Journal of the American Statistical Association*, 90, 1277–1288.
- (2007), “Spatial variation of total column ozone on a global scale,” *Annals of Applied Statistics*, 1, 191–210.
- Wikle, C. K. and Cressie, N. (1999), “A dimension-reduction approach to space-time Kalman filtering,” *Biometrika*, 86, 815–829.
- Zhang, H. and Zimmerman, D. L. (2005), “Towards reconciling two asymptotic frameworks in spatial statistics,” *Biometrika*, 92, 921–936.

Table 1. Empirical sizes (%) of the test of stationarity using subsampling for the spatial case in Section 4.1.

m	c	20×20			40×40		
		Two lags	Four lags	Eight lags	Two lags	Four lags	Eight lags
2	0.5	3.3	5.2	7.8	2.8	3.3	4.4
	1.0	2.4	5.2	1.4	1.0	3.0	6.0
	1.5	3.3	1.8	3.3	1.0	2.3	10.2
5	0.5	10.8	7.0	7.8	13	4.7	3.7
	1.0	6.5	4.7	9.1	8.4	2.7	3.0
	1.5	10.8	12.2	23.3	4.0	2.4	5.6
8	0.5	24.7	9.3	10.6	24.7	8.3	5.7
	1.0	19.3	8.6	9.2	18.6	2.9	3.2
	1.5	18.8	15.3	17.4	13.1	5.4	5.4

NOTE: Nominal level is 5%. Empirical sizes are calculated based on 1000 simulations and the largest standard error for sizes is 1.6%. Here m is the range of spatial dependence in (11) and the c values of 0.5, 1, and 1.5 correspond to the subblock size 2×2 , 4×4 , and 7×7 for 20×20 grids and 3×3 , 6×6 , and 9×9 for 40×40 grids.

Table 2. Empirical powers (%) of the test of stationarity using subsampling for the spatial case in Section 4.1.

c	20×20			40×40		
	Two lags	Four lags	Eight lags	Two lags	Four lags	Eight lags
.5	41.8	39.6	36.0	98.5	97.6	98.6
1.0	33.8	36.1	44.8	95.9	95.9	95.2
1.5	29.5	43.8	55.8	91.2	88.3	92.4

NOTE: Nominal level is 5%. Empirical powers are calculated based on 1000 simulations and the largest standard error for powers is 1.6%. The value of c is defined in Table 1.

Table 3. Empirical sizes (%) and powers (%) of the test of axial symmetry and stationarity in time using subsampling for the spatial case in Section 4.2.

split	$l(n)$	SIZE		POWER	
		Λ_1	Λ_2	Λ_1	Λ_2
longitude	5	6.2	2.0	6.3	1.9
	10	6.5	5.2	6.5	5.2
	20	7.9	11.2	8.0	11.0
latitude	5	6.4	6.6	90.5	66.3
	10	6.6	11.7	90.5	69.6
	20	8.1	19.2	90.5	72.7

NOTE: Nominal level is 5%. Empirical sizes and powers are calculated based on 1000 simulations and 130 random splits are performed. The largest standard error for sizes is 1.2% and that for powers is 1.5%. The size of subblock is $l(n)$.

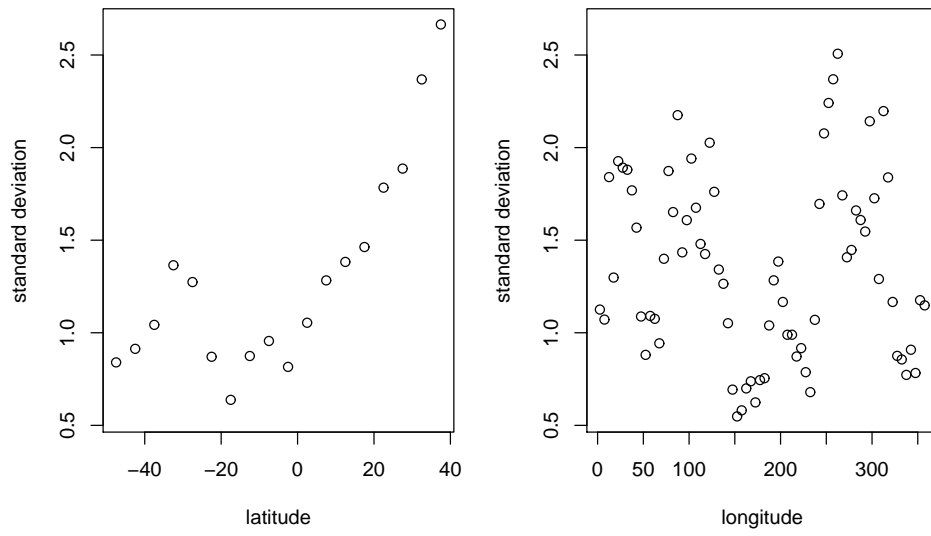
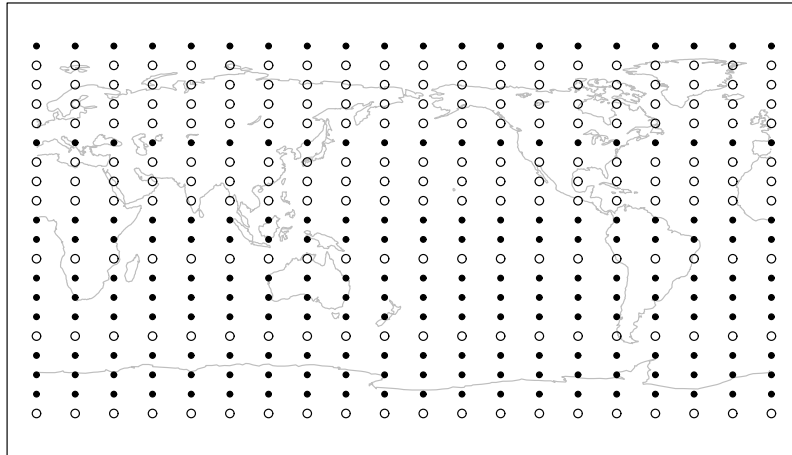


Figure 1. Standard deviations for the global surface temperature data (monthly average) in December, 1999, with respect to latitude (left panel) and longitude (right panel).

split wrt latitude



split wrt longitude

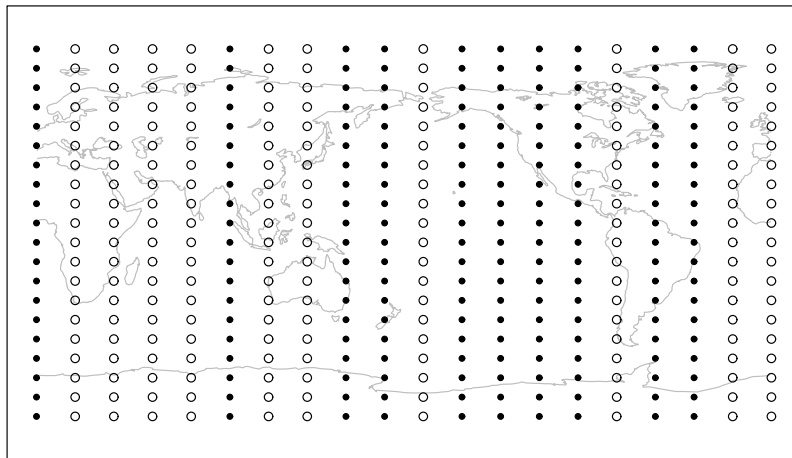


Figure 2. Example of two ways of splitting the spherical domain.

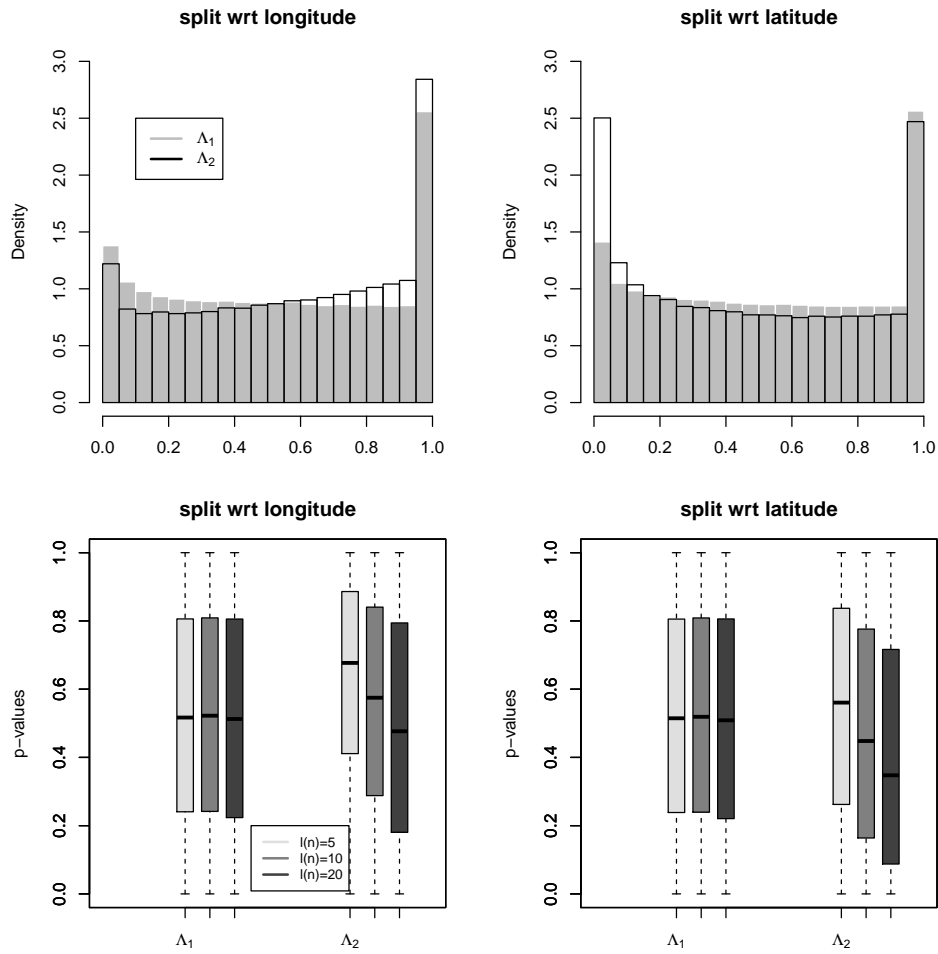


Figure 3. P-values from the test with the simulated data in Section 4.2. Histograms are based on 1000 simulations and 130 random splits for all the subblock sizes altogether. Boxplots are different for different subblock sizes. For the definitions on Λ_1, Λ_2 and $l(n)$, see Section 4.2.

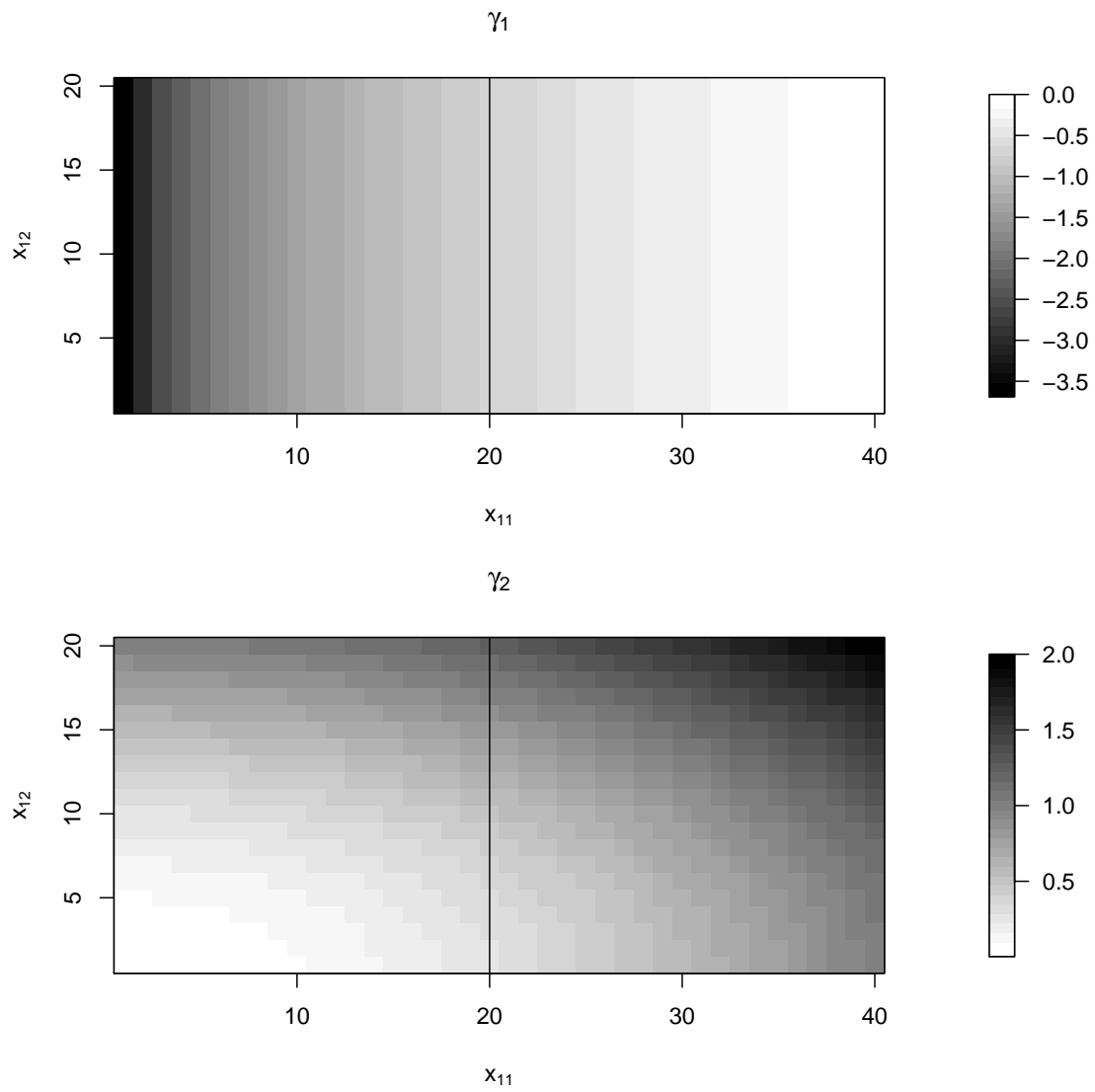


Figure 4. Image plots of the functions γ_1 and γ_2 over two adjacent 20×20 spatial grids used to generate Σ_1 and Σ_2 in (12) in Section 4.1.

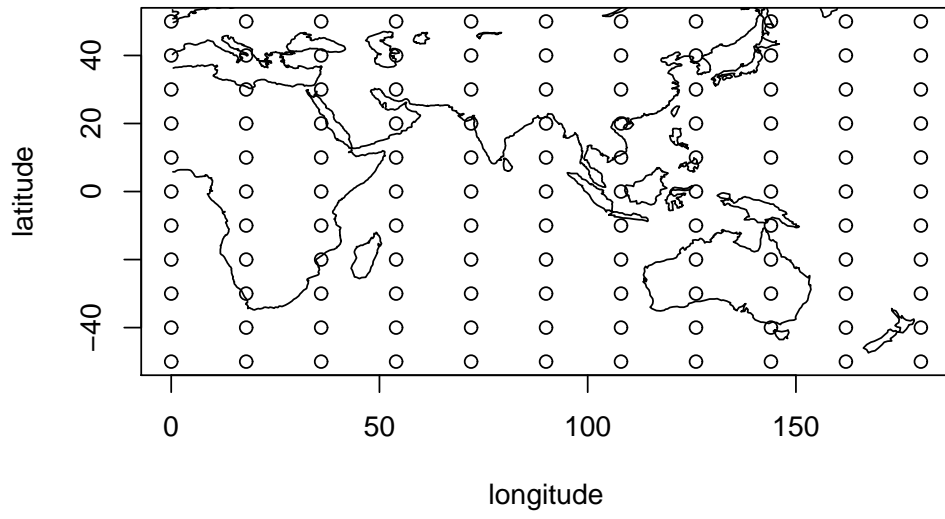


Figure 5. Locations on the sphere for the simulation in Section 4.2.

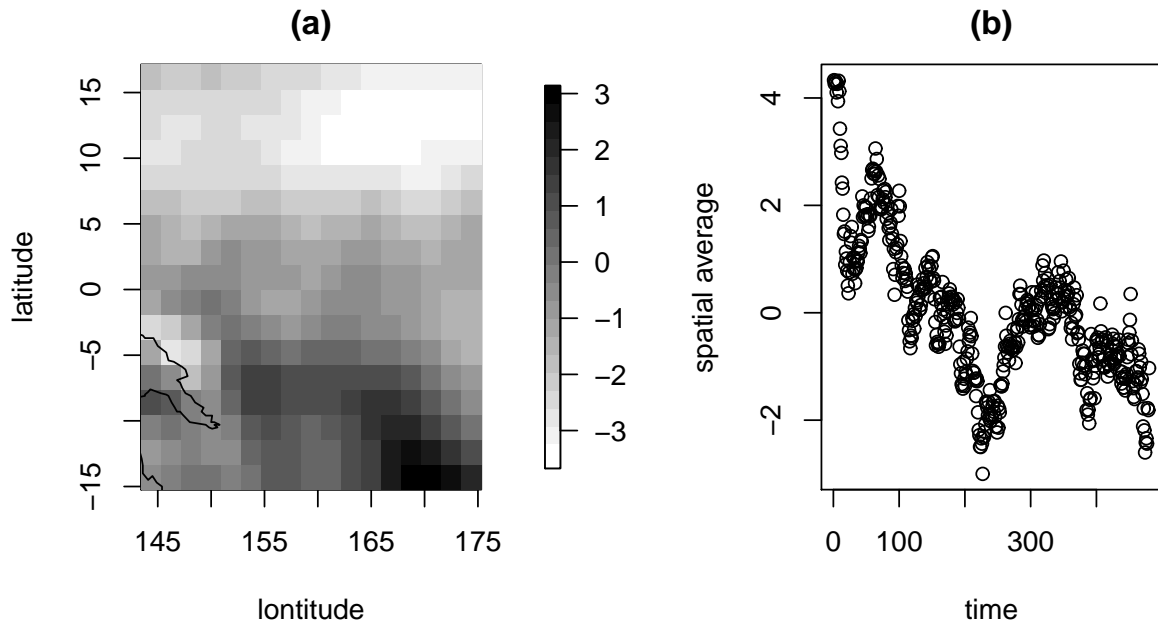


Figure 6. (a): temporal average of the raw wind speed data (b): spatial average of the wind speed after removing temporal average from the raw data.

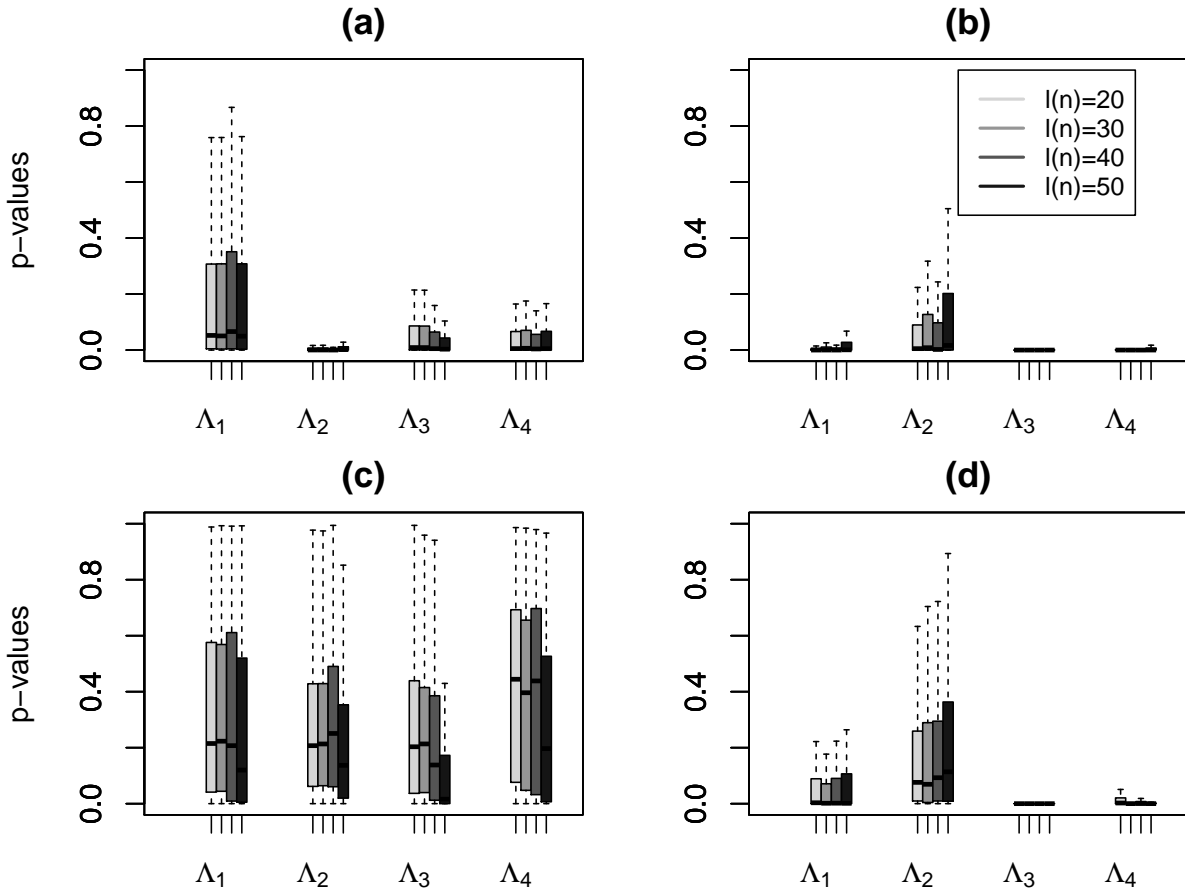


Figure 7. Boxplots of p-values for the tests with the wind data in Section 5.1 based on 1000 random splitting of the domains. (a): results on the raw data after removing the grand mean, with the split with respect to longitude (b): same data as (a), with the split with respect to latitude (c): results on the data after removing both spatial and temporal average, with the split with respect to longitude (d): same data as (c), with the split with respect to latitude. The subblock size is $l(n)$.

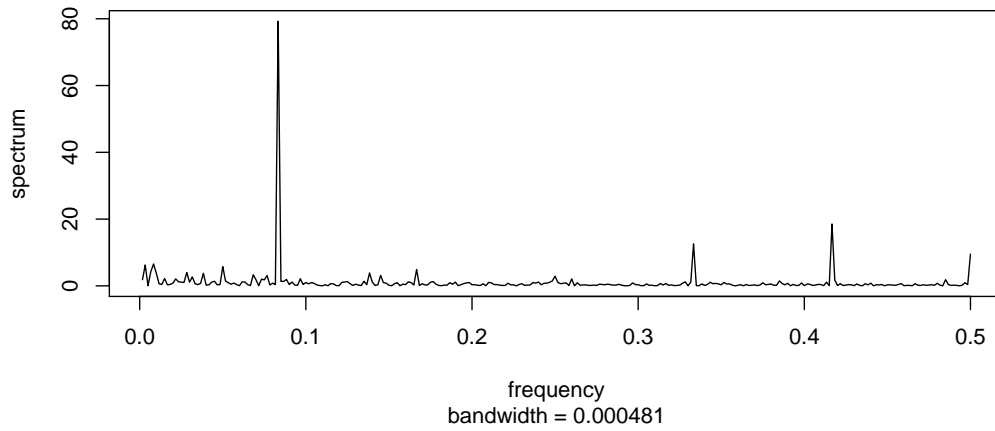


Figure 8. Raw periodogram of “diff” time series at spatial location 47.5° S and 47.5° E.

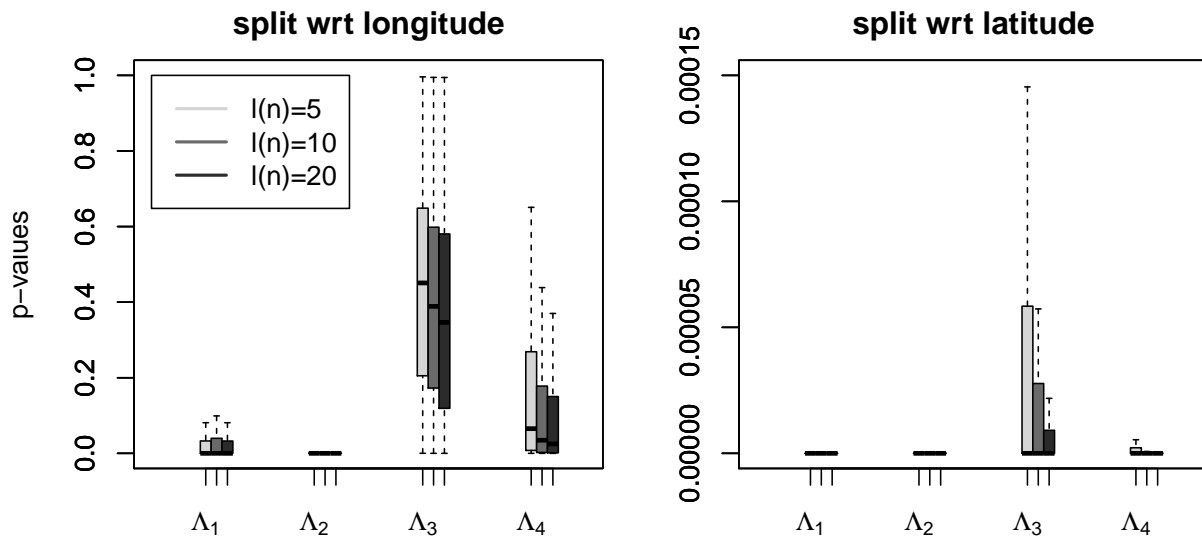


Figure 9. Boxplots of p -values for the tests with the “diff” process in Section 5.2. The distributions of p -values are generated from 1000 random splitting of the longitude and latitude and $l(n)$ indicates different sizes of subblocks used in subsampling. Notice the different scales of the y -axis for the two figures.